NOTE **Communicated by William Lytton**

A Simple Model of Transmitter Release and Facilitation

Richard Bertram
Pennsylvania State University, Division of Science,
Erie, PA 16563 USA

We describe a model of synaptic transmitter release and presynaptic facilitation that is based on activation of release sites by single Ca^{2+} microdomains. Facilitation is due to Ca^{2+} that remains bound to release sites between impulses. This model is inherently stochastic, but deterministic equations can be derived for the mean release. The number of equations required to describe the mean release is small, so it is practical to use the model with models of neuronal electrical activity to investigate the effects of different input spike patterns on presynaptic facilitation. We use it in conjunction with a model of dopamine-secreting neurons of the basal ganglia to demonstrate that transmitter release is greater when the neuron bursts than when it spikes continuously, due to the greater facilitation generated by the bursting impulse pattern. Finally, a minimal form of the model is described that is coupled to simple models of postsynaptic receptors and passive membrane to compute the postsynaptic voltage response to a train of presynaptic stimuli. This form of the model is appropriate for neural network simulations.

1 Introduction

Several models have been proposed for synaptic transmitter release and presynaptic facilitation, the process whereby impulse-evoked release is enhanced for up to several hundred milliseconds if preceded by one or more conditioning impulses (Magleby, 1987). In the models of Zucker and Fogelson (1986) and Yamada and Zucker (1992), release sites and Ca^{2+} channels are spatially separated, and facilitation is due primarily to residual free Ca^{2+} left over from previous impulse-induced Ca^{2+} channel openings, so the diffusion of free Ca^{2+} is important. In an alternative model (Stanley, 1986; Bertram, Sherman, & Stanley, 1996), each transmitter release site is colocalized with a single Ca^{2+} channel. Release is then activated by the microdomain of Ca^{2+} surrounding the channel mouth, eliminating the need to perform Ca^{2+} diffusion calculations. This model is intended to describe release evoked by short depolarizations, such as action potentials, during which the opening of multiple Ca^{2+} channels in the neighborhood of a release site is unlikely.

In the single-domain model, each release site has four independent Ca^{2+} binding sites or gates, each of which must be bound for release to occur. Kinetics of the gates are graded from slow unbinding, high affinity to fast unbinding, low affinity. Facilitation is due to the accumulation of Ca^{2+} bound to one or more of the gates rather than to residual free Ca^{2+}. This model was motivated by the findings that release sites can be activated by the Ca^{2+} microdomain under a single channel (Stanley, 1993) and that there is a steplike frequency dependence of facilitation associated with a steplike decline of Ca^{2+} cooperativity (Stanley, 1986). There is also considerable evidence that residual free Ca^{2+} does not play an important role in facilitation (Stanley, 1986; Blundon, Wright, Brodwick, & Bittner, 1993; Winslow, Duffy, & Charlton, 1994), although it does appear to play a role in other forms of enhancement that last for several seconds (augmentation) or several minutes (posttetanic potentiation) following a high-frequency conditioning tetanus (Delaney, Zucker, & Tank, 1989; Delaney & Tank, 1994).

2 The Mathematical Model

The binding of Ca^{2+} to the jth gate obeys a first-order kinetic scheme:

$$U_j + Ca \underset{k_j^-}{\overset{k_j^+}{\rightleftharpoons}} B_j\,, \quad j = 1, 2, 3, 4, \tag{2.1}$$

where B_j and U_j are the normalized ($B_j + U_j = 1$) concentrations or probabilities of bound and unbound gates and Ca is the concentration of free Ca^{2+} at the release site. The binding rates (k_j^+, in $\text{msec}^{-1}\mu\text{M}^{-1}$) and unbinding rates ($k_j^-$, in msec^{-1}) were chosen to produce steps in the facilitation curve: $k_1^+ = 3.75 \times 10^{-3}$, $k_1^- = 4 \times 10^{-4}$, $k_2^+ = 2.5 \times 10^{-3}$, $k_2^- = 1 \times 10^{-3}$, $k_3^+ = 5 \times 10^{-4}$, $k_3^- = 0.1$, $k_4^+ = 7.5 \times 10^{-3}$, $k_4^- = 10$. The k_j^- vary from small to large, resulting in a wide range of unbinding time constants ($1/k_j^-$): 2.5 sec, 1 sec, 10 msec, and 0.1 msec, respectively. The temporal evolution of B_j is described by

$$\frac{dB_j}{dt} = -(k_j^- + k_j^+ Ca)\, B_j + k_j^+ Ca\,, \quad j = 1, 2, 3, 4. \tag{2.2}$$

The opening and closing of a Ca^{2+} channel is a stochastic process, with transition rates that depend on membrane voltage (V). The quantity Ca is therefore a random variable. In Bertram et al. (1996), a Monte Carlo procedure was used to handle the effects of stochastic channel activity on release. Although effective, this approach is computationally demanding, and a better approach was subsequently developed (Bertram & Sherman, in press). Here, Fokker-Planck-type partial differential equations were derived for the probability distributions of bound gates under open and closed

Ca^{2+} channels. Ordinary differential equations for the expected values of these distributions—that is, the mean concentrations of bound gates of each type—were then derived. Although the four gates are physically independent, they are statistically correlated through their common dependence on the domain Ca^{2+} concentration. Therefore, expected or mean release is not simply the product of the mean bound concentrations of each gate type; it depends on the mean concentrations of all gate configurations, resulting in a system of 30 differential equations. However, it was shown that the correlation among gates is removed and the number of equations necessary to compute release reduced to 4 if it is assumed that the gates respond to the *average* domain Ca^{2+} concentration—the domain Ca^{2+} concentration averaged over the entire population of Ca^{2+} channels. Using perturbation analysis, it was shown that the error introduced by this approximation is typically small.

Taking the expected values of both sides of equation 2.2, and replacing $\mathrm{E}[Ca\,B_j]$ by $\mathrm{E}[Ca]\,\mathrm{E}[B_j]$ (the average domain Ca^{2+} approximation), we get

$$\frac{d\sigma_j}{dt} = -(k_j^- + k_j^+ \overline{Ca})\,\sigma_j + k_j^+ \overline{Ca}\,, \quad j = 1, 2, 3, 4, \tag{2.3}$$

where σ_j is the expected value of B_j and $\overline{Ca} = \mathrm{E}[Ca]$ is the average domain Ca^{2+} concentration, equal to the product of the fraction of open channels (m) and the domain Ca^{2+} concentration at an open channel (Ca_{open}). The latter is assumed to be proportional to the Ca^{2+} influx through an open channel ($i(V)$): $Ca_{\mathrm{open}} = -A\,i(V)$. Assuming that the Ca^{2+} channel has a single open and a single closed state, the fraction of open channels satisfies

$$\frac{dm}{dt} = \alpha_m\,(1 - m) - \beta_m\,m \tag{2.4}$$

where α_m, β_m are the channel opening and closing rates, respectively. Expected release is then

$$\mathrm{E}[R] = \sigma_1\,\sigma_2\,\sigma_3\,\sigma_4. \tag{2.5}$$

The fourth gate, unlike the others, has fast unbinding kinetics, so that σ_4 changes rapidly with changes in $\overline{Ca}$. Thus, the number of differential equations needed to compute $\mathrm{E}[R]$ is further reduced by one by assuming that σ_4 is in equilibrium with $\overline{Ca}$.

3 Example: The Dopamine Neuron

Our release model can be used with any model of membrane voltage or even with experimental voltage recordings. As an example, we use it in

conjunction with a model of in vitro electrical activity of the dopamine neuron of the basal ganglia (Li, Bertram, & Rinzel, 1996). A periodic bursting pattern, high-frequency spiking followed by a long period of silence, is produced (see Fig. 1B) in the presence of the glutamate agonist N-methyl-D-aspartate (NMDA). In the absence of NMDA, the cell spikes continuously at a lower frequency (see Fig. 1A). Mean release evoked by the continuous spiking pattern shows some facilitation (see Fig. 1E), due to the slow growth of σ_1 and σ_2 (see Fig. 1C). However, facilitation generated by the bursting pattern is much greater (see Fig. 1F), consistent with in vivo experimental findings (Gonon, 1988). In this case σ_3 increases during the first portion of the active phase, while σ_1 and σ_2 increase throughout the active phase (see Fig. 1D), facilitating release within an active phase. Between active phases σ_3 decays back to its baseline value, but the burst period is short enough (800 msec) that the active-phase increases in σ_1 and σ_2 are not entirely lost. Therefore, σ_1 and σ_2 accumulate over several bursts, and release evoked by later bursts is greater than that evoked by earlier ones.

4 A Minimal Model

To demonstrate how the transmitter release model can be used in neural network simulations, it is simplified to a form that can be used with integrate-and-fire neurons. This model is coupled to simple models of postsynaptic transmitter receptors and passive membrane to generate a postsynaptic voltage response. Following Destexhe, Mainen, & Sejnowski (1994a) we assume that each impulse leads to the release of a square pulse of transmitter of 1 msec duration. In contrast to Destexhe et al., we assume that the size of the transmitter pulse evoked by each stimulus is not constant. The magnitude of the initial pulse is $T^{(1)}$, while the magnitude of each subsequent pulse is the product of $T^{(1)}$ and the presynaptic facilitation. Facilitation is computed by solving equation 2.3 for σ_1, σ_2, and σ_3 (or just one of the three for the simplest model that exhibits facilitation) assuming that each presynaptic stimulus leads to a square pulse of $\overline{Ca}$ lasting 1 msec. (With 10 mM external Ca^{2+}, $\overline{Ca}$ summed over an impulse is 63 μM, using the Hodgkin-Huxley equations [Hodgkin & Huxley, 1952] to generate the impulse. This value may be used as the magnitude of the $\overline{Ca}$ pulse, scaled linearly to reflect any changes in the external Ca^{2+} concentration.) Facilitation contributed by the jth gate is then the ratio of σ_j at the end of the nth pulse to the value at the end of the first pulse.

We assume that the facilitating transmitter pulses act on a simple two-state postsynaptic receptor (Destexhe et al., 1994a), with the fraction of bound receptors (a) given by

$$\frac{da}{dt} = \alpha_a T (1 - a) - \beta_a a, \tag{4.1}$$

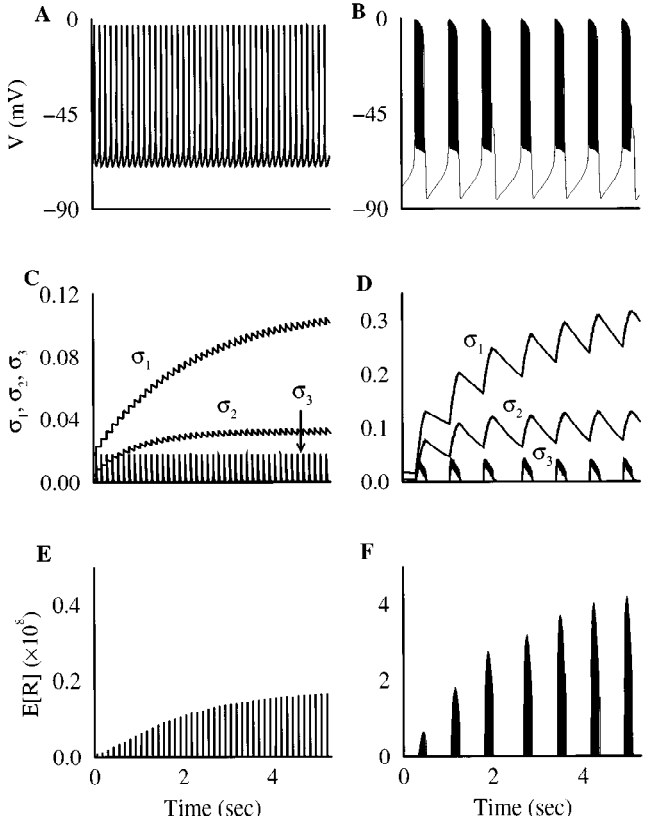

Figure 1: Expected release (see equations 2.3–2.5) evoked by a dopamine neuron model. In the presence of NMDA, the cell generates bursts of action potentials (B); otherwise, it spikes continuously (A). Release is much greater when the cell bursts (E, F; notice the different scales) due to the greater accumulation of bound gates (C, D; σ_3 has been multiplied by 30). The single-channel Ca^{2+} current is given by a Goldman-Hodgkin-Katz expression, $i(V) = 1.45V[Ca_{ex}/(1 - \exp(0.07V))]$, where $Ca_{ex} = 1$ mM is the external Ca^{2+} concentration. We use $A = 0.1\ \mu\text{M fA}^{-1}$ and $\alpha_m = 3.1\,e^{V/10}$, $\beta_m = e^{-V/26.7}$ to compute $\overline{Ca}$. Both α_m and β_m are based on squid giant synapse data (Llinás, Steinberg, & Walton, 1981) modified for the higher temperature at which dopamine neurons typically operate (37°F).

where T is the transmitter concentration and α_a and β_a are the binding and unbinding rates, respectively. Postsynaptic membrane voltage (V_{post}) is computed with the passive membrane equation

$$\frac{dV_{\text{post}}}{dt} = -(I_{\text{mem}} + I_{\text{syn}}) / C_{\text{mem}} \tag{4.2}$$

where C_{mem} is the membrane capacitance, $I_{\text{mem}} = \bar{g}_{\text{mem}} (V - V_{\text{mem}})$ is the passive membrane current, and $I_{\text{syn}} = \bar{g}_{\text{syn}} a (V - V_{\text{syn}})$ is the synaptic current. Note that since both $\overline{Ca}$ and T appear as square pulses in equations 2.3 and 4.1, the equations have piecewise exponential solutions (see Destexhe et al., 1994a).

In Figure 2 this minimal model is used to compute the postsynaptic voltage response to a short 100-Hz stimulus train. The synapse facilitates throughout the train, producing consistently larger transmitter pulses (see Fig. 2A) and postsynaptic voltage depolarizations (see Fig. 2B). Combined with the relatively slow membrane dynamics, this leads to a substantial rise in the average postsynaptic voltage (see Fig. 2B, solid curve). In contrast, when facilitation is excluded by assuming that the size of each transmitter pulse is the same, the average postsynaptic voltage exhibits only a small rise, associated with the slow membrane dynamics (see Fig. 2B, dashed curve).

5 Discussion

Computational models of synaptic transmission typically concentrate on postsynaptic mechanisms, assuming explicitly or implicitly that the amount of neurotransmitter released by each impulse is the same (Rall, 1967; Destexhe et al., 1994a). However, a key feature of the transmission process is that the number of transmitter molecules released by an impluse depends on the history of presynaptic electrical activity. The model discussed here is one of several intended to describe presynaptic transmitter release and short-term presynaptic enhancement (Zucker & Fogelson, 1986; Parnas, Dudel, & Parneas, 1986; Yamada & Zucker, 1992). In addition to the differences discussed earlier, these other release models differ from the present one in the structure of their release sites. In Zucker and Fogelson (1986), it was assumed that the kinetics of Ca^{2+} binding to a release site are instantaneous, so that the rate of release is proportional to some power of the Ca^{2+} concentration at the release site. This model was later modified to include finite kinetic rates (Yamada & Zucker, 1992), but because the modified model includes only one slow Ca^{2+} binding site, facilitation depends largely on residual-free Ca^{2+}, contrary to a growing body of experimental data (Stanley, 1986; Blundon et al., 1993; Winslow et al., 1994). In addition, this model does not account for the multiple time scales of facilitation observed experimentally (Stanley, 1986; Magleby, 1987). Finally, the model by Parnas et al. (1986)

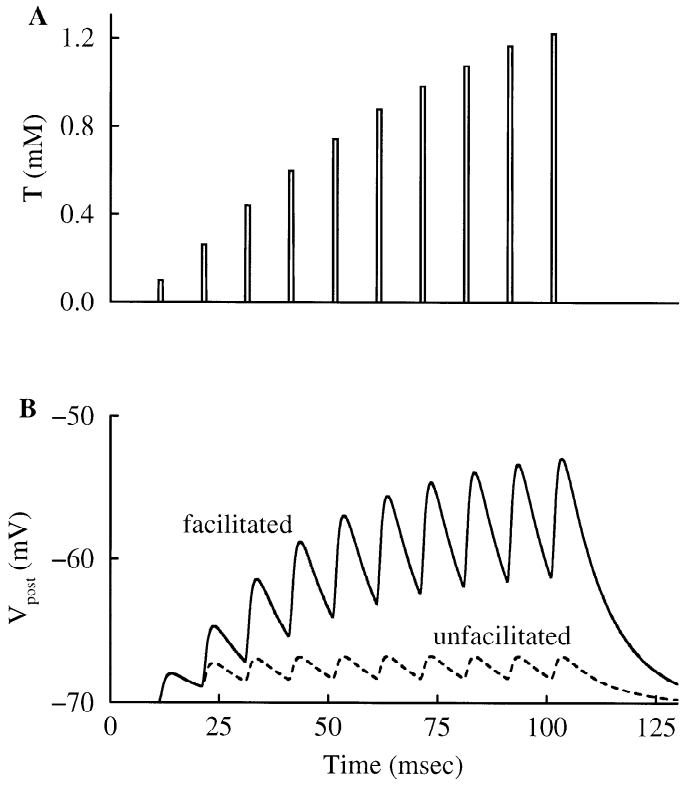

Figure 2: The minimal model of presynaptic facilitation is combined with simple models of postsynaptic binding and passive membrane to describe the postsynaptic voltage response to a short 100-Hz impulse train (see equations 2.3, 4.1, and 4.2). (A) Each stimulus elicits a 1-msec square pulse of transmitter (T). The magnitude of the first pulse is assumed to be 0.1 mM. The magnitude of subsequent pulses grows as the synapse facilitates. (B) The increased magnitude of T results in an increased postsynaptic voltage response with each stimulus, leading to a significant rise in the average postsynaptic voltage (solid line). In the absence of facilitation, the average voltage equilibrates at a lower level (dashed line). Postsynaptic parameter values are: $\alpha_a = 2\ \text{msec}^{-1}\,\text{mM}^{-1}$, $\beta_a = 1\ \text{msec}^{-1}$, $\bar{g}_{\text{mem}} = 0.1$, $\bar{g}_{\text{syn}} = 0.2\ (\mu\text{M}\,\text{cm}^{-2})$, $V_{\text{mem}} = -70$, $V_{\text{syn}} = 0\ (\text{mV})$, and $C_{\text{mem}} = 1\,\mu\text{F}\,\text{cm}^{-2}$.

postulates an explicit voltage dependence in the release mechanism, a feature that has not been supported by experimental data (Landò & Zucker, 1994).

The present model also belongs to the family of kinetic models used to describe a wide variety of neuronal mechanisms (see Destexhe, Mainen, & Sejnowski, 1994b, for an overview). These include voltage-gated and ligand-gated ion channels (Hodgkin & Huxley, 1952; Destexhe et al., 1994b); IP_3-sensitive Ca^{2+} channels in the membrane of the endoplasmic reticulum (De Young & Keizer, 1992); postsynaptic receptors and channels (Standley, Ramsey, & Usherwood, 1993; Destexhe et al., 1994a,b); and presynaptic transmitter release sites (Parnas et al., 1986; Yamada & Zucker, 1992; Destexhe et al., 1994b; Bertram et al., 1996). In Destexhe et al. (1994b) a nonfacilitating kinetic model of transmitter release was coupled to kinetic models of postsynaptic receptor binding to provide a description of the complete synaptic signal transduction process. As demonstrated in Figure 2, the release model discussed in this article can be applied in a similar manner, introducing the key feature of presynaptic facilitation to the signal transduction scheme.

Acknowledgments

I thank Arthur Sherman for many helpful discussions and for a careful reading of the manuscript. This work was performed while I was at the Mathematical Research Branch (NIDDK, NIH) in Bethesda, MD.

References

Bertram, R., and Sherman, A. (In press). Population dynamics of synaptic release sites, *SIAM J. Appl. Math.*

Bertram, R., Sherman, A., and Stanley, E. F. (1996). Single-domain/bound calcium hypothesis of transmitter release and facilitation. *J. Neurophysiol., 75*, 1919–1931.

Blundon, J. A., Wright, S. N., Brodwick, M. S., and Bittner, G. D. (1993). Residual free calcium is not responsible for facilitation of neurotransmitter release. *Proc. Natl. Acad. Sci. USA, 90*, 9388–9392.

De Young, G., and Keizer, J. (1992). A single pool IP_3-receptor based model for agonist stimulated Ca^{2+} oscillations. *Proc. Natl. Acad. Sci. USA, 89*, 9895–9899.

Delaney, K. R., and Tank, D. W. (1994). A quantitative measurement of the dependence of short-term synaptic enhancement on presynaptic residual calcium. *J. Neurosci., 14*, 5885–5902.

Delaney, K. R., Zucker, R. S., and Tank, D. W. (1989). Calcium in motor nerve terminals associated with posttetanic potentiation. *J. Neurosci., 9*, 3558–3567.

Destexhe, A., Mainen, Z. F., and Sejnowski, T. J. (1994a). An efficient method for computing synaptic conductances based on a kinetic model of receptor binding. *Neural Computation, 6*, 14–18.

Destexhe, A., Mainen, Z. F., and Sejnowski, T. J. (1994b). Synthesis of models for excitable membranes, synaptic transmission and neuromodulation using a common kinetic formalism. *J. Comput. Neurosci., 1*, 195–230.

Gonon, F. G. (1988). Nonlinear relationship between impulse flow and dopamine release by rat midbrain dopaminergic neurons as studied by in vivo electrochemistry. *Neuroscience, 24*, 19–28.

Hodgkin, A. L., and Huxley, A. F. (1952). A quantitative description of membrane current and its application to conduction and excitation in nerve. *J. Physiol. (Lond.), 117*, 500–544.

Landò, L., and Zucker, R. S. (1994). Ca^{2+} cooperativity in neurosecretion measured using photolabile Ca^{2+} chelators. *J. Neurophysiol., 72*, 825–830.

Li, Y.-X., Bertram, R., and Rinzel, J. (1996). Modeling N-methyl-D-aspartate-induced bursting in dopamine neurons. *Neuroscience, 71*, 397–410.

Llinás, R., Steinberg, I. Z., and Walton, K. (1981). Presynaptic calcium currents in squid giant synapse. *Biophys. J., 33*, 289–322.

Magleby, K. (1987). Short-term changes in synaptic efficacy. In G. M. Edelman, L. E. Gall, W. Maxwell, & W. M. Cowan (Eds.), *Synaptic Function*, (pp. 21–56). New York: Wiley.

Parnas, H., Dudel, J., and Parnas, I. (1986). Neurotransmitter release and its facilitation in the crayfish. VII. Another voltage dependent process besides Ca entry controls the time course of phasic release. *Pflügers Arch., 406*, 121–130.

Rall, W. (1967). Distinguishing theoretical synaptic potentials computed for different somadendritic distributions of synaptic inputs. *J. Neurophysiol., 30*, 1138–1168.

Standley, C., Ramsey, R. L., and Usherwood, P. N. R. (1993). Gating kinetics of the quisqualate-sensitive glutamate receptor of locust muscle studied using agonist concentration jumps and computer simulations. *Biophys. J., 65*, 1379–1386.

Stanley, E. F. (1986). Decline in calcium cooperativity as the basis of facilitation at the squid giant synapse. *J. Neurosci., 6*, 782–789.

Stanley, E. F. (1993). Single calcium channels and acetylcholine release at a presynaptic nerve terminal. *Neuron, 11*, 1007–1011.

Winslow, J. L., Duffy, S. N., and Charlton, M. P. (1994). Homosynaptic facilitation of transmitter release in crayfish is not affected by mobile calcium chelators: Implications for the residual ionized calcium hypothesis from electrophysiological and computational analyses. *J. Neurophysiol., 72*, 1769–1793.

Yamada, W. M., and Zucker, R. S. (1992). Time course of transmitter release calculated from simulations of a calcium diffusion model. *Biophys. J., 61*, 671–682.

Zucker, R. S., and Fogelson, A. L. (1986). Relationship between transmitter release and presynaptic calcium influx when calcium enters through discrete channels. *Proc. Natl. Acad. Sci. USA, 83*, 3032–3036.

Received April 10, 1996; accepted August 9, 1996.